

# Measurement of polarization-transfer to bound protons in carbon and its virtuality dependence

D. Izraeli<sup>a,1,\*</sup>, T. Breceelj<sup>b,1</sup>, P. Achenbach<sup>c</sup>, A. Ashkenazi<sup>a</sup>, R. Böhm<sup>c</sup>, E.O. Cohen<sup>a</sup>, M.O. Distler<sup>c</sup>, A. Esser<sup>c</sup>, R. Gilman<sup>d</sup>, T. Kolar<sup>b</sup>, I. Korover<sup>a,e</sup>, J. Lichtenstadt<sup>a</sup>, I. Mardor<sup>a,f</sup>, H. Merkel<sup>c</sup>, M. Mihovilović<sup>b,c</sup>, U. Müller<sup>c</sup>, M. Olivenboim<sup>a</sup>, E. Piasezky<sup>a</sup>, G. Ron<sup>g</sup>, B.S. Schlimme<sup>c</sup>, M. Schoth<sup>c</sup>, C. Sfienti<sup>c</sup>, S. Širca<sup>h,b</sup>, S. Štajner<sup>b</sup>, S. Strauch<sup>i</sup>, M. Thiel<sup>c</sup>, A. Weber<sup>c</sup>, I. Yaron<sup>a</sup>,

(A1 Collaboration)

<sup>a</sup>*School of Physics and Astronomy, Tel Aviv University, Tel Aviv 69978, Israel.*

<sup>b</sup>*Jožef Stefan Institute, 1000 Ljubljana, Slovenia.*

<sup>c</sup>*Institut für Kernphysik, Johannes Gutenberg-Universität, 55099 Mainz, Germany.*

<sup>d</sup>*Rutgers, The State University of New Jersey, Piscataway, NJ 08855, USA.*

<sup>e</sup>*Department of Physics, NRCN, P.O. Box 9001, Beer-Sheva 84190, Israel.*

<sup>f</sup>*Soreq NRC, Yavne 81800, Israel.*

<sup>g</sup>*Racah Institute of Physics, Hebrew University of Jerusalem, Jerusalem 91904, Israel.*

<sup>h</sup>*Faculty of Mathematics and Physics, University of Ljubljana, 1000 Ljubljana, Slovenia.*

<sup>i</sup>*University of South Carolina, Columbia, South Carolina 29208, USA.*

arXiv:1711.09680v2 [nucl-ex] 16 Feb 2018

## Abstract

We measured the ratio  $P_x/P_z$  of the transverse to longitudinal components of polarization transferred from electrons to bound protons in  $^{12}\text{C}$  by the  $^{12}\text{C}(\vec{e}, e'\vec{p})$  process at the Mainz Microtron (MAMI). We observed consistent deviations from unity of this ratio normalized to the free-proton ratio,  $(P_x/P_z)_{^{12}\text{C}}/(P_x/P_z)_{^1\text{H}}$ , for both  $s$ - and  $p$ -shell knocked out protons, even though they are embedded in averaged local densities that differ by about a factor of two. The dependence of the double ratio on proton virtuality is similar to the one for knocked out protons from  $^2\text{H}$  and  $^4\text{He}$ , suggesting a universal behavior. It further implies no dependence on average local nuclear density.

Deviations of quasi-elastic measurements on nuclei from those performed on protons or from calculations using free-proton form-factors (FFs) reflect various many-body effects, potentially including medium modifications of the bound proton structure in the nuclear field [1, 2]. The ratio of the transverse ( $P_x$ ) to longitudinal ( $P_z$ ) polarization transfer components measured in the elastic double-polarized process  $^1\text{H}(\vec{e}, e'\vec{p})$  is proportional to the ratio of the electric to magnetic FFs of the free proton,  $R_{^1\text{H}} \equiv (P_x/P_z)_{^1\text{H}} \propto G_E^p/G_M^p$  [3]. In nuclei, the ratio of the polarization transfer components to a bound proton,  $R_A \equiv (P_x/P_z)_A$ , can be determined from the analogous quasi-free proton knock-out process  $A(\vec{e}, e'\vec{p})$ . Measurements of  $R_A$  eliminate many systematic uncertainties and thus constitute a sensitive and precise tool to study possible deviations of a bound proton properties from a free one.

Previous double polarized proton knock-out experiments on light nuclei,  $^2\text{H}$  and  $^4\text{He}$ , were found to be in agreement when compared in terms of the proton virtuality, which is a measure of the “off-shellness” of the bound proton (see Eq. (2)). The measurements showed no dependence on the average nuclear density nor on momentum transfer [4]. For the deuteron, detailed calculations [5] explained the devia-

tions from the free proton by final state interactions (FSI). It is thus interesting to extend the measurements to heavier nuclei where FSI effects are expected to be different.

The  $^{12}\text{C}$  nucleus is a particularly appealing target for such studies as one can selectively probe protons from specific nuclear shells,  $s$  and  $p$ . The average local densities in these shells differ by about a factor of two, which was predicted to impact the polarization transfer to  $s$ - and  $p$ -shell protons differently [6]. Previous measurements on  $s$ - and  $p$ -shell protons in  $^{16}\text{O}$  were limited in statistics and the kinematical range covered [7].

In this paper we report on the measurements of the  $P_x/P_z$  ratio for protons bound in carbon,  $^{12}\text{C}(\vec{e}, e'\vec{p})$ , and present the double ratio  $R_{^{12}\text{C}}/R_{^1\text{H}}$ . In terms of virtuality, our results exhibit consistency between  $s$ - and  $p$ -shell protons as well as with measurements obtained on other light nuclei. Thus, they confirm the absence of average nuclear density dependence even in the heavier nucleus  $^{12}\text{C}$ .

The experiment was performed at the Mainz Microtron (MAMI) accelerator using the A1 beam-line and spectrometers [8]. We used a 600 MeV continuous-wave polarized electron beam with a current of about 10  $\mu\text{A}$ . The average beam polarization was about 80%, measured with a Møller polarimeter and verified by Mott polarimetry. The uncertainty in the beam polarization was less than 5%. The beam helicity was flipped at a rate of 1 Hz. Two high-resolution, small solid-angle spectrometers with momentum

\*Corresponding author

Email address: davidizraeli@post.tau.ac.il (D. Izraeli)

<sup>1</sup>These authors contributed equally to this work.

Table 1: The kinematic settings in the experiment. The angles and momenta represent the central values for the two spectrometers:  $p_p$  and  $\theta_p$  ( $p_e$  and  $\theta_e$ ) are the knocked out proton (scattered electron) momentum and scattering angles, respectively.

Kinematic	Setting	
	A	B
$Q^2$ [GeV <sup>2</sup> /c <sup>2</sup> ]	0.40	0.18
$p_{\text{miss}}$ [MeV/c]	-130 to 100	-250 to -100
$p_e$ [MeV/c]	385	368
$\theta_e$ [deg]	82.4	52.9
$p_p$ [MeV/c]	668	665
$\theta_p$ [deg]	-34.7	-37.8
# of events after cuts	1.7 M	1.1 M

acceptances of 20 – 25% were used to detect the scattered electrons in coincidence with the knocked-out protons. The target consisted of three carbon foils of 0.8 mm thickness each, separated by about 1.5 cm and tilted at an angle of 40° with respect to the beam. The usage of three tilted foils reduced the proton energy loss in the target and improved the resolution for the reaction-vertex determination. This reduced the systematic uncertainty in the determined polarization transfer components at the reaction point. The proton spectrometer was equipped with a polarimeter placed behind its focal-plane (FPP) using a 7 cm thick carbon analyzer [8, 9]. The spin-dependent scattering of the polarized proton by the carbon analyzer enables the determination of the proton transverse polarization components at the focal plane [9]. The polarization-transfer components at the reaction point were obtained by correcting the measured components for the spin precession in the magnetic field of the spectrometer. Following the convention of [2], both  $P_z$  and  $P_x$  were determined in the scattering plane, defined by the incident and scattered electron momenta, where  $P_z$  is along and  $P_x$  is perpendicular to the momentum transfer vector,  $\vec{q}$ .

In the analysis, cuts were applied to identify coincident electrons and protons that originate from the carbon target, and to ensure good reconstruction of tracks in the spectrometers and the FPP. To remove Coulomb scattering events by the carbon analyzer, we selected only events that scattered by more than 8° in the FPP.

The polarization transfer components  $P_x$  and  $P_z$  were first determined as a function of the proton missing momentum defined as  $\vec{p}_{\text{miss}} = \vec{q} - \vec{p}_p$ , where  $\vec{p}_p$  is the outgoing proton momentum. We define the scalar missing momentum,  $p_{\text{miss}} \equiv \pm |\vec{p}_{\text{miss}}|$ , where the sign is taken to be positive (negative) if the longitudinal component of  $\vec{p}_{\text{miss}}$  is parallel (anti-parallel) to  $\vec{q}$ . The measurements were performed in two kinematical settings that covered two ranges in  $p_{\text{miss}}$  and two ranges in the invariant four-momentum transfer  $Q^2 = \vec{q}^2 - \omega^2$ , where  $\omega$  is the energy transfer. Details of the kinematics are summarized in Table 1.

The protons knocked out from the  $s$  and  $p$  shells were identified by their missing energy. The missing energy is defined as  $E_{\text{miss}} \equiv \omega - T_p - T_{11\text{B}}$ , where  $T_p$  is the mea-

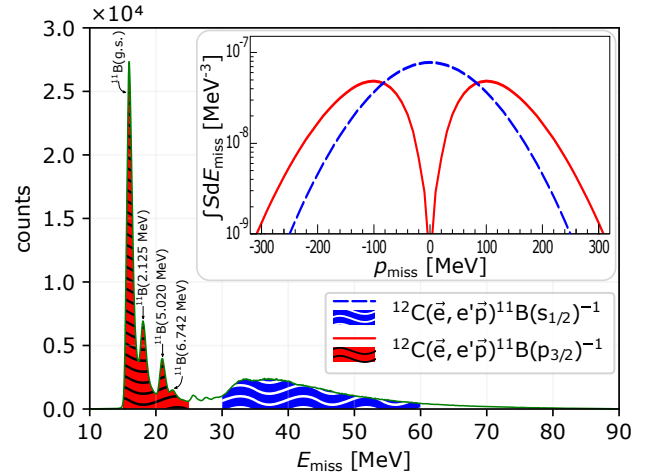


Figure 1: The proton missing energy spectrum for  $^{12}\text{C}(e, e'p)$  in setup A. The distinct peaks correspond to removal of  $p_{3/2}$ -shell protons in  $^{12}\text{C}$  resulting in  $^{11}\text{B}$  ground state and excited states as noted. The  $E_{\text{miss}}$  ranges considered in the analysis for  $p_{3/2}$  and  $s_{1/2}$  protons are marked in red and blue, respectively. The green line denotes the  $E_{\text{miss}}$  range used for the analysis combining all protons. The inset shows the momentum distribution predictions of the independent particle shell model for  $p_{3/2}$  and  $s_{1/2}$  protons in  $^{12}\text{C}$ , obtained from [10].

sured kinetic energy of the outgoing proton, and  $T_{11\text{B}}$  is the calculated kinetic energy of a recoiling  $^{11}\text{B}$  nucleus (g.s.). The missing-energy spectrum of setting A is shown in Fig. 1. The sharp peaks correspond to the ground state and the lowest excited states of the recoiling  $^{11}\text{B}$ . Following Dutta *et al.* [10] we present the polarization-transfer results for two ranges of  $E_{\text{miss}}$  shown in the figure: the first ( $15 < E_{\text{miss}} < 25$  MeV) corresponds to proton removal primarily from the  $^{12}\text{C}$   $p_{3/2}$  shell; the second ( $30 < E_{\text{miss}} < 60$  MeV) corresponds predominantly to proton removal from the  $s$ -shell. The missing energy cut allows some  $s$ -shell strength in the  $p$ -shell region and vice versa. In addition, we show the combined data from the entire  $E_{\text{miss}}$  range ( $10 < E_{\text{miss}} < 90$  MeV) covering proton removal from both  $s$ - and  $p$ -shells. The inset in Fig. 1 (adapted from [10]), shows the predicted momentum distributions of  $p$ - and  $s$ -shell protons in  $^{12}\text{C}$  obtained from an independent particle shell model spectral function (S) [10]. The difference between the  $s$ - and  $p$ -shell proton momentum distributions around  $p_{\text{miss}} = 0$ , may impact the polarization transfer in this region.

Helicity-independent uncertainties in the measured ratios (acceptance, detector efficiency, target density, etc.) largely cancel out due to frequent flips of the beam helicity. The uncertainties in beam polarization, carbon analyzing power and efficiency are reduced well below the statistical uncertainty by taking the  $P_x/P_z$  ratio. The total systematic uncertainty in  $R_{12\text{C}}$ , dominated by the vertex position reconstruction in the target, does not exceed 2% and is about 25% of the statistical uncertainty. In the following figures, only the statistical uncertainties are shown.

The measured helicity-dependent ratios  $R_{12\text{C}}$  for both settings are presented in Fig. 2 (top) as a function of  $p_{\text{miss}}$ . The difference in  $R_{12\text{C}}$  between  $s$ - and  $p$ -shell proton re-

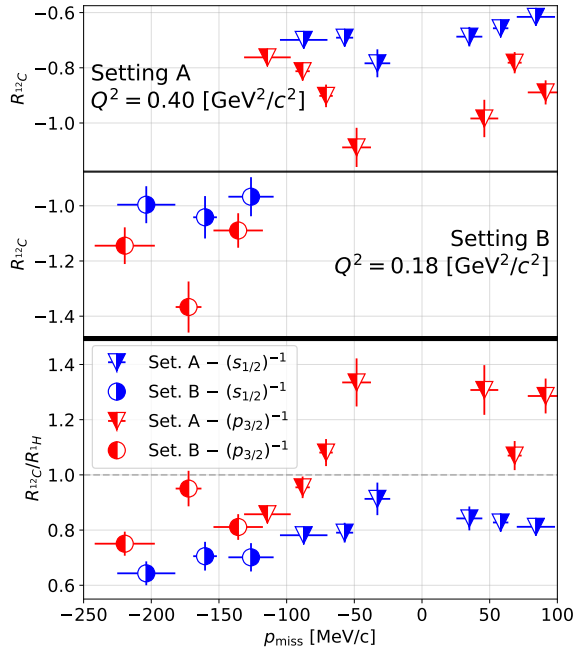


Figure 2: The measured ratio of polarization transfer components,  $R_{12C}$  (top) and the double ratio  $R_{12C}/R_{1H}$  (bottom), versus the missing-momentum. The measurements for  $p_{3/2}$ - and  $s_{1/2}$ -shell protons are shown separately. The uncertainties are statistical only, and the horizontal bars indicate the width of the  $p_{\text{miss}}$  distribution in each bin (standard deviation). The legend is common to all panels in the figure. Note, triangles (circles) refer to kinematical setting A (B). Symbols open on the left (right) side refer to  $s$ - ( $p$ -) shell removals.

removal with the same  $p_{\text{miss}}$  is clearly visible in the figure. We removed some contributions to the differences between data at the same  $p_{\text{miss}}$ , which are due to the different kinematics (or momentum transfer), by dividing  $R_{12C}$  by the hydrogen ratio

$$R_{1H} \equiv \left( \frac{P_x}{P_z} \right)_{1H} = - \frac{2M_p c^2}{(E + E') \tan \frac{\theta_e}{2}} \cdot \frac{G_E^p(Q^2)}{G_M^p(Q^2)}, \quad (1)$$

where  $E$  is the incident electron energy, and  $M_p$  is the proton mass. The scattered electron energy ( $E' = E' (E, Q^2)$ ) and scattering angle ( $\theta_e = \theta_e (E, Q^2)$ ) are calculated assuming elastic electron-proton scattering.

$R_{1H}$  was calculated on an event by event basis using the proton FFs parametrized by Bernauer et al. [11] and averaged over the bin. The double-ratio of the  $^{12}\text{C}$  data to  $^1\text{H}$ ,  $R_{12C}/R_{1H}$ , is shown in the bottom panel of Fig. 2. However, even after division by  $R_{1H}$ , the differences between  $s$ - and  $p$ -shell results at the same missing momenta are still significant.

The bound nucleon can be characterized also by its virtuality, i.e. its ‘‘off-shellness’’. There is no unique way to define virtuality. Following [4] we define the virtuality,  $\nu$ , of a bound proton as

$$\nu \equiv \left( M_A c - \sqrt{M_{A-1}^2 c^2 + p_{\text{miss}}^2} \right)^2 - p_{\text{miss}}^2 - M_p^2 c^2, \quad (2)$$

where  $M_A$  is the mass of the target nucleus,  $M_{A-1} \equiv$

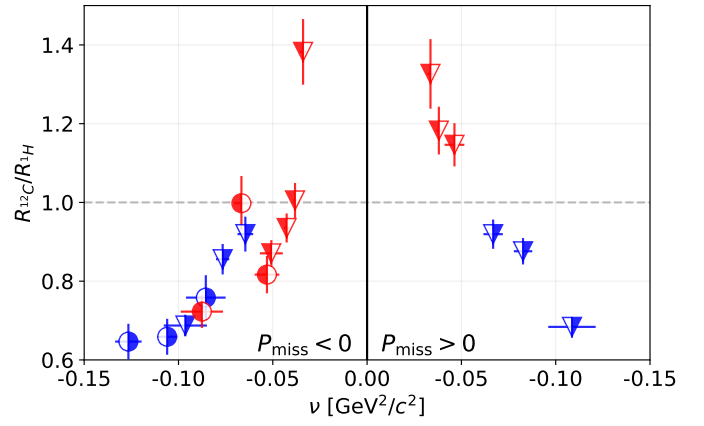


Figure 3: The measured double-ratio,  $R_{12C}/R_{1H}$ , for  $p$ - and  $s$ -shell protons, as a function of the proton virtuality. The virtuality dependence is shown separately for positive and negative missing momenta. We used the same symbols as in Fig. 2.

$\sqrt{(\omega - E_p + M_A)^2 - p_{\text{miss}}^2}$  (determined event by event), and  $E_p$  is the total energy of the outgoing proton. We note that the virtuality (Eq. (2)) is not a unique function of  $p_{\text{miss}}$ . This is demonstrated in the two dimensional event distribution of  $\nu$  vs  $p_{\text{miss}}$  shown in the supplementary material [12]. Equation (2) implies that the struck proton is off-shell ( $\neq M_p^2 c^2$ ) and the recoil system is on-shell. The virtuality dependence of  $R_{12C}/R_{1H}$  is shown in Fig. 3. The double ratios are shown separately for positive and negative missing momenta due to possible differences, as observed in  $^4\text{He}$  [2] and calculated for  $^2\text{H}$  due to FSI [4].

The  $s$ - and  $p$ -shell protons have different wave functions as reflected also in their missing-momentum distributions. These differences, such as the behavior at  $p_{\text{miss}} = 0$  (see [10] and Fig. 1) and possibly the total angular momentum, may affect the polarization transfer, as predicted by calculations [13, 14]. Nevertheless, the corresponding double-ratios have the same smooth behavior, and show the same virtuality dependence, as is clearly shown in Fig. 3. Motivated by the observed good agreement between the  $s$ - and  $p$ -shell protons as a function of virtuality, we combined the data and obtained  $R_{12C}/R_{1H}$  for the entire missing energy region,  $10 < E_{\text{miss}} < 90$  MeV.

In Fig. 4, the  $^{12}\text{C}$  double ratios, combined for  $s$ - and  $p$ -shell proton removals, are compared with those of  $^2\text{H}$  obtained at MAMI for the same kinematics [4], as well as to  $^2\text{H}$  and  $^4\text{He}$  data measured at JLab at  $Q^2 = 1$  and  $0.8 \text{ GeV}^2/c^2$ , respectively [2, 15]. Note that the data shown in Fig. 4 are not identical to those in Fig. 3 due to the different  $E_{\text{miss}}$  range and bins. The new  $^{12}\text{C}$  data almost double the virtuality range covered by the data from light nuclei. The higher values of  $R_{12C}/R_{1H}$  at  $|\nu| < 0.04 \text{ GeV}^2/c^2$  are due to  $p_{3/2}$  protons whose behavior is attributed to the  $p$  wave function properties at small  $|p_{\text{miss}}|$  [13, 14], unlike  $s$ -shell protons in the other nuclei.

The data suggest that the double-ratio is characterized well by the virtuality of the struck proton. Virtuality seems to be a better parameter than  $p_{\text{miss}}$  to describe polarization

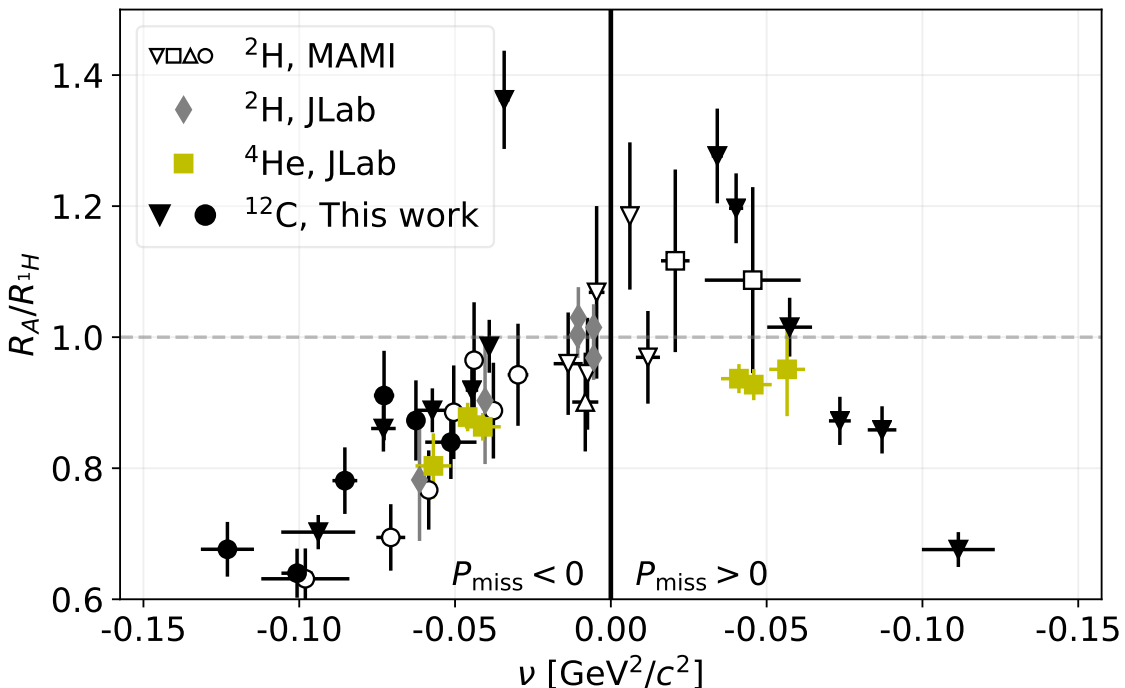


Figure 4: The measured double-ratio of protons from  $^{12}\text{C}$  compared with those obtained for  $^2\text{H}$  and  $^4\text{He}$  ( $R_A/R_{1H}$ ,  $A = ^2\text{H}, ^4\text{He}, ^{12}\text{C}$ ) as a function of the proton virtuality. The  $^{12}\text{C}$  data (black full symbols) are the combined  $s$ - and  $p$ -shell removal of this work. The open symbols are  $^2\text{H}$  data measured at Mainz [4] with essentially the same kinematics as the present work [4]. The light symbols are  $^2\text{H}$  and  $^4\text{He}$  data measured at JLab at  $Q^2 = 1$  and  $0.8 \text{ GeV}^2/c^2$ , respectively [2, 15]. The triangles (circles) refer to setting A (B) as in Fig. 2.

transfer to a struck proton in different nuclei.

To test this hypothesis, we compared the  $^{12}\text{C}$  data to the MAMI  $^2\text{H}$  data. To enable an event-by-event comparison, we adjusted the theoretical calculations [5] for  $^2\text{H}$  to reproduce the measured polarization transfer components of  $^2\text{H}$ . The ratio of the  $^{12}\text{C}$  data to the adjusted model is  $1.07 \pm 0.03$ . In this comparison we excluded the afore mentioned  $|\nu| < 0.04 \text{ GeV}^2/c^2$  data, due to its special behavior.

The agreement between the data from the different nuclei suggests that the observed deviations from the free proton ratio have a common origin. We note that Eq. (1) is valid only for a free proton. Thus the double ratio in nuclei does not remove FSI effects. When the deuteron data [4] were compared to the calculations of [5], the theory was in good agreement with the data. This implies that in the deuteron most of the deviation is due to FSI. One may speculate that the same effects dominate in heavier nuclei as well, although this has to be confirmed by detailed calculations. These should take into account the variation of the kinematics over the experimental phase space. Such a task is rather involved and may depend on various parameters. The new  $^{12}\text{C}$  data may provide important information for determination of the mechanisms at work and the validity of using free proton FFs in such calculations.

The data confirm that the virtuality of the struck proton is the preferred parameter for comparing the deviations from a free proton. This implies that further measurements to look for local nuclear density effects should compare polarization transfer to protons at different local densities, like different shells, but with the same virtuality as can be de-

duced from Fig. 3. This comparison requires high statistics in order to confirm or reject in medium modification of the proton FFs, which are estimated at a few percent [6].

To summarize, our data of the polarization-transfer ratios for  $^{12}\text{C}$  extend the previous nuclear measurements on  $^2\text{H}$  and almost double the virtuality range. The new double ratios  $R_{12\text{C}}/R_{1\text{H}}$  agree well with those previously measured on  $^2\text{H}$  and  $^4\text{He}$ , including those obtained in different kinematics. The double-ratios exhibit a similar shape for nuclei with very different average local density. The new results suggest also that measurements of both  $^2\text{H}$  and  $^4\text{He}$  over an extended virtuality range are needed. Indeed, such measurements were proposed [16] and approved at JLab.

We would like to thank the Mainz Microtron operators and technical crew for the excellent operation of the accelerator. This work is supported by the Israel Science Foundation (Grant 390/15) of the Israel Academy of Arts and Sciences, by the Israel Ministry of Science, Technology and Space, by the Deutsche Forschungsgemeinschaft with the Collaborative Research Center 1044, by the U.S. National Science Foundation (PHY-1205782), and by the Croatian Science Foundation Project No. 1680. We acknowledge the financial support from the Slovenian Research Agency (research core funding No. P1-0102).

## References

- [1] S. Dieterich, et al., Polarization transfer in the  ${}^4\text{He}(\vec{e}, e'\vec{p}){}^3\text{H}$  reaction, *Physics Letters B* 500 (1–2) (2001) 47 – 52. doi:[10.1016/S0370-2693\(01\)00052-1](https://doi.org/10.1016/S0370-2693(01)00052-1).
- [2] S. Strauch, et al., Polarization transfer in the  ${}^4\text{He}(\vec{e}, e'\vec{p}){}^3\text{H}$  reaction up to  $Q^2 = 2.6$  (GeV/c) $^2$ , *Phys. Rev. Lett.* 91 (2003) 052301. doi:[10.1103/PhysRevLett.91.052301](https://doi.org/10.1103/PhysRevLett.91.052301).
- [3] A. I. Akhiezer, M. Rekalov, Polarization effects in the scattering of leptons by hadrons, *Sov. J. Part. Nucl.* 4 (1974) 277, [*Fiz. Elem. Chast. Atom. Yadra*4,662(1973)].
- [4] I. Yaron, D. Izraeli, et al., Polarization-transfer measurement to a large-virtuality bound proton in the deuteron, *Physics Letters B* 769 (2017) 21 – 24. doi:[10.1016/j.physletb.2017.01.034](https://doi.org/10.1016/j.physletb.2017.01.034).
- [5] H. Arenhövel, W. Leidemann, E. L. Tomusiak, General survey of polarization observables in deuteron electrodisintegration, *Eur. Phys. J. A*23 (2005) 147–190. doi:[10.1140/epja/i2004-10061-5](https://doi.org/10.1140/epja/i2004-10061-5).
- [6] G. Ron, W. Cosyn, E. Piasetzky, J. Ryckebusch, J. Lichtenstadt, Nuclear density dependence of in-medium polarization, *Phys. Rev. C* 87 (2013) 028202. doi:[10.1103/PhysRevC.87.028202](https://doi.org/10.1103/PhysRevC.87.028202).
- [7] S. Malov, et al., Polarization transfer in the  ${}^{16}\text{O}(\vec{e}, e'\vec{p}){}^{15}\text{N}$  reaction, *Phys. Rev. C* 62 (2000) 057302. doi:[10.1103/PhysRevC.62.057302](https://doi.org/10.1103/PhysRevC.62.057302).
- [8] K. Blomqvist, et al., The three-spectrometer facility at MAMI, *Nucl. Instrum. and Meth. A* 403 (2–3) (1998) 263 – 301. doi:[10.1016/S0168-9002\(97\)01133-9](https://doi.org/10.1016/S0168-9002(97)01133-9).
- [9] T. Pospischil, et al., The focal plane proton-polarimeter for the 3-spectrometer setup at MAMI, *Nucl. Instrum. Methods. Phys. Res., Sect. A* 483 (3) (2002) 713 – 725. doi:[10.1016/S0168-9002\(01\)01955-6](https://doi.org/10.1016/S0168-9002(01)01955-6).
- [10] D. Dutta, et al., Quasielastic ( $e, e'p$ ) reaction on  ${}^{12}\text{C}$ ,  ${}^{56}\text{Fe}$ , and  ${}^{197}\text{Au}$ , *Phys. Rev. C* 68 (2003) 064603. doi:[10.1103/PhysRevC.68.064603](https://doi.org/10.1103/PhysRevC.68.064603).
- [11] J. C. Bernauer, et al., Electric and magnetic form factors of the proton, *Phys. Rev. C*90 (1) (2014) 015206. doi:[10.1103/PhysRevC.90.015206](https://doi.org/10.1103/PhysRevC.90.015206).
- [12] D. Izraeli, T. Brecej, et al., Supplemental material.
- [13] J. Ryckebusch, D. Debruyne, W. Van Nispen, S. Janssen, Meson and isobar degrees of freedom in ( $\vec{e}, e'\vec{p}$ ) reactions at  $0.2 < Q^2 < 0.8$  (GeV/c) $^2$ , *Phys. Rev. C* 60 (1999) 034604. doi:[10.1103/PhysRevC.60.034604](https://doi.org/10.1103/PhysRevC.60.034604).
- [14] C. Giusti, J. Ryckebusch, private communication (2017).
- [15] B. Hu, et al., Polarization transfer in the  ${}^2\text{H}(\vec{e}, e'\vec{p})n$  reaction up to  $Q^2 = 1.61$  (GeV/c) $^2$ , *Phys. Rev. C*73 (2006) 064004. doi:[10.1103/PhysRevC.73.064004](https://doi.org/10.1103/PhysRevC.73.064004).
- [16] S. Strauch, E. Brash, G. Huber, R. Ransome, Jefferson Lab experiment E12-11-002.



# Measurement of polarization-transfer to bound protons in carbon and its virtuality dependence

D. Izraeli<sup>a,1</sup>, T. Brecej<sup>b,1</sup>, *et al.*

<sup>a</sup>*School of Physics and Astronomy, Tel Aviv University, Tel Aviv 69978, Israel.*

<sup>b</sup>*Jožef Stefan Institute, 1000 Ljubljana, Slovenia.*

---

## Abstract

Supplementary material.

---

The virtuality as defined in the main text is shown in Fig. S1 versus the missing momentum calculated on an event by event basis. The distinct peaks in Fig. 1, corresponding to removal of  $p_{3/2}$ -shell protons from  $^{12}\text{C}$  that result in  $^{11}\text{B}$  ground state and excited states are well identified, leading to different virtuality for the same  $p_{\text{miss}}$ . The events considered in the analysis for  $p_{3/2}$  and  $s_{1/2}$  protons are marked in red and blue, respectively.

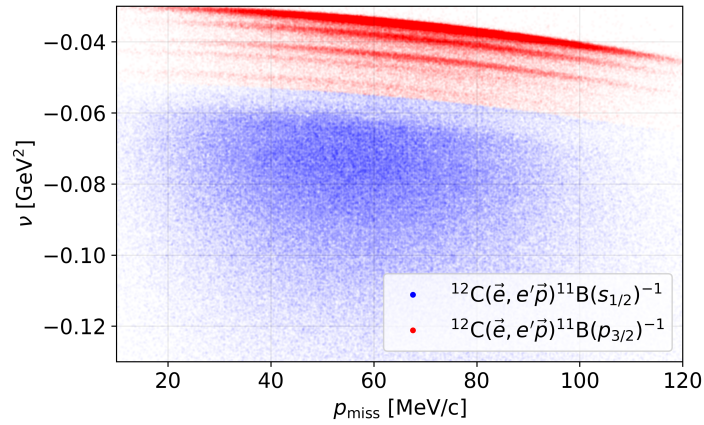


Figure S1: The virtuality versus the missing momentum calculated on an event by event basis.

---

<sup>1</sup>These authors contributed equally to this work.